

Interchangeable Role of Motor Cortex and Reafference for the Stable Execution of an Orofacial Action

Michael A. Elbaz,¹ Maxime Demers,¹ David Kleinfeld,^{2,3} Christian Ethier,¹ and Martin Deschênes¹

¹CERVO Brain Research Center, Laval University, Québec City, Québec G1J 2G3, Canada, ²Departments of Physics, and ³Neurobiology, University of California, San Diego, La Jolla, California 92093

Animals interact with their environment through mechanically active, mobile sensors. The efficient use of these sensory organs implies the ability to track their position; otherwise, perceptual stability or prehension would be profoundly impeded. The nervous system may keep track of the position of a sensorimotor organ via two complementary feedback mechanisms—peripheral reafference (external, sensory feedback) and efference copy (internal feedback). Yet, the potential contributions of these mechanisms remain largely unexplored. By training male rats to place one of their vibrissae within a predetermined angular range without contact, a task that depends on knowledge of vibrissa position relative to their face, we found that peripheral reafference is not required. The presence of motor cortex is not required either, except in the absence of peripheral reafference to maintain motor stability. Finally, the red nucleus, which receives descending inputs from motor cortex and cerebellum and projects to facial motoneurons, is critically involved in the execution of the vibrissa positioning task. All told, our results point toward the existence of an internal model that requires either peripheral reafference or motor cortex to optimally drive voluntary motion.

Key words: efference copy; internal model; motor cortex; red nucleus; sensorimotor; vibrissa; whisker

Significance Statement

How does an animal know where a mechanically active, mobile sensor lies relative to its body? We address this basic question in sensorimotor integration using the motion of the vibrissae in rats. We show that rats can learn to reliably position their vibrissae in the absence of sensory feedback or in the absence of motor cortex. Yet, when both sensory feedback and motor cortex are absent, motor precision is degraded. This suggests the existence of an internal model able to operate in closed- and open-loop modes, requiring either motor cortex or sensory feedback to maintain motor stability.

Introduction

Decoding information gathered through moving sensors, the hallmark of active sensing, requires keeping track of the position of the sensors (Connolly and Goodale, 1999; Wolpert and Ghahramani, 2000; Kleinfeld and Deschênes, 2011; Wurtz, 2018). The exploratory motor action of the vibrissae in rodents instantiates this faculty for haptic sensation. Indeed, mice and rats can report the location of an

object in their vibrissa field with great precision (Knutsen et al., 2006; Mehta et al., 2007; O'Connor et al., 2010), which implies that they know the position of their vibrissae with respect to their face, at least during touch (Cheung et al., 2019). Two non-exclusive mechanisms may account for knowledge of vibrissa position, namely, internal feedback via efference copy and sensory feedback via peripheral reafference (Wolpert et al., 1995; Fee et al., 1997; Wolpert and Ghahramani, 2000). With efference copy, an internal copy of motor-related neural processes allows the brain to keep track of the consequences of its motor commands (Crapse and Sommer, 2008). With reafferent signals, sensory receptors encode the position of the organ or the kinematics of the ongoing movement (Fee et al., 1997; Severson et al., 2017, 2019). Although previous studies established that both mechanisms are plausible at different anatomic levels of the vibrissa system (Hill et al., 2011; Moore et al., 2015b; Chen et al., 2016; Severson et al., 2017, 2019), their ethological value remains unknown.

Vibrissa tasks involving touch are not suited for disentangling the role of efference copy and reafferent signals for two reasons. First, primary vibrissa afferents multiplex exafferent (touch) and reafferent (self-motion) signals (Moore et al., 2015b; Gutnisky et

Received Oct. 31, 2022; revised June 25, 2023; accepted June 27, 2023.

Author contributions: M.A.E., C.E., and M. Deschênes designed research; M.A.E. and M. Demers performed research; M.A.E., D.K., and C.E. analyzed data; M.A.E. wrote the paper.

This work was supported by Canadian Institutes of Health Research Grant MT-5877 and the National Institutes of Health Grants U19 NS107466 and U01 NS090595. We thank Ehud Ahissar (Weizmann Institute of Science) and David Golomb (Ben-Gurion University) for discussions, Andrew Miri (Northwestern University) and Windsor Ting (Laval University) for comments on the manuscript, Sergiu Ftomov (Laval University) for technical help, and Julia Kuhl and Gabrielle Lahaye for preparing illustrations.

M.A. Elbaz's present address: Department of Neurobiology, Northwestern University, Evanston, Illinois 60208.

The authors declare no competing financial interests.

Correspondence should be addressed to Michaël A. Elbaz at mielbaz@gmail.com or Martin Deschênes at martin.deschenes@fmed.ulaval.ca.

<https://doi.org/10.1523/JNEUROSCI.2089-22.2023>

Copyright © 2023 the authors

al., 2017; Severson et al., 2017, 2019), which makes it essentially impossible to manipulate reafferent signals without interfering with exafferent signals. Second, in the somatosensory cortex, a region that is required to localize objects with vibrissae (O'Connor et al., 2010; Guo et al., 2014), there is a continuous transformation of sensory and efference copy signals along sensorimotor loops (Kleinfeld et al., 1999; Ahissar and Kleinfeld, 2003; Veinante and Deschênes, 2003; Mao et al., 2011; Petreanu et al., 2012) that blurs their respective contribution. To circumvent these limitations, we designed a vibrissa positioning task that implicitly requires knowledge of vibrissa position or a surrogate of position such as muscle activation. Critically, the task does not involve touch and is conducted in the dark. Thus, the sensory information at play consists solely of reafferent signals that can be experimentally manipulated (Fee et al., 1997).

Materials and Methods

The protocol for this study was approved by the Comité de Protection des Animaux de l'Université Laval. All procedures were conducted in strict accordance with the Canadian animal care and use guidelines. All surgical procedures were performed under ketamine-xylazine anesthesia.

Animals

Seventeen Long-Evans male rats (Charles River Laboratories), 250–350 g in mass, were used for combined behavioral, neurophysiological, and anatomic experiments. They were housed in a reverse dark/light cycle in a facility with controlled temperature and humidity. After a week of daily handling aimed at getting them habituated to the experimental room and to the experimenter, they were implanted with a plate for head fixation, following procedures previously described (Moore et al., 2015a). A week after head-plate implantation, the rats were placed under water restriction. They were head restrained over increased periods of time and given water concomitantly. After being habituated and comfortable enough to drink sufficient water while being head restrained (10 ml/100 g body weight/day), we began exposing them to the vibrissa positioning task (referred to hereafter as “the task”). From that moment on, all their vibrissae but left C1 (Brecht et al., 1997) were trimmed weekly under light isoflurane anesthesia to optimize the online detection of the vibrissa of interest and to prevent tactile contact with any element of the surrounding environment. The choice of C1 was motivated by the relatively stable dorsoventral level of this vibrissa along its whole retraction-protraction range, which results in an azimuthal motion. Rats were trained to the task twice a day, with 20 min per session and at least 4 h apart between both sessions, from Monday to Friday.

Vibrissa positioning task

All behavioral experiments were conducted with head-restrained rats in a silent and dark room under near infrared illumination (880 nm). The task was implemented with custom MATLAB (MathWorks) scripts operating two cameras; one was used as a lickometer to detect tongue movements and the other to detect vibrissa position with respect to the head anteroposterior axis, that is, monitoring the absolute vibrissa angle.

Task trials were self-initiated by the rat when its C1 vibrissa was detected in the go zone (70–90° with respect to the head axis; Fig. 1a). Trial onset was accompanied by an auditory cue (4 kHz, 300 ms), from which the rat had 10 s to position its vibrissa in the reward zone (100–130°) and maintain the positioning for a given required hold time. Over training, the required hold time increased from 10 ms up to 1 s (for one animal, up to 2 s) in an adaptive fashion that depended on the success rate of previous active trials. An active trial is defined as a trial during which the vibrissa went 5° beyond the upper limit of the go zone, that is, beyond 95°. When the mean success rate of the 50 past active trials reached 50%, the hold time was increased by 5% of its previous value, up to the expert level value (1 s or for one animal, 2 s). At the end of each trial, a 1 or 8 kHz auditory signal (300 ms), respectively, indicated

whether the trial was successful or unsuccessful. In case of success, a pump was activated to deliver 75 µl of water. After a successful trial, a pause of variable duration (5–8 s), during which it was not possible to initiate another trial, allowed animals to lick the delivered water without interfering with the task. After an unsuccessful trial, there was a 1 s pause to prevent the juxtaposition of trials in case the vibrissa was in the go zone when the failed trial ended. Distinct audio sounds were then played to announce the end of the failed trial and the onset of the following trial, respectively. Rats that did not reach a hold time higher than 200 ms within a training period of 4 weeks were excluded from this study.

Adaptation protocols

With the first adaptation protocol, when the mean success rate of the 50 past active trials reached 50%, the upper limit of the reward zone, initially at 130°, was lowered by 1° increments, down to a minimum of 110°.

With the second adaptation protocol, each rat was tested for at least two sessions for each of two reward zones (100–110° and 105–115°) alternatively (e.g., session 1, 100–110°; session 2, 105–115°; session 3, 100–110°, etc.).

Deafferentation

On the side of the tracked vibrissa (left), we transected the infraorbital (sensory) branch of the infraorbital nerve at its entrance in the orbit (Berg and Kleinfeld, 2003). On the opposite side (right), we transected the branches of the facial motor nerve innervating the musculature of the mystacial pad (namely, the buccal and marginal branches; Fee et al., 1997; Henstrom et al., 2012). Thus, the mystacial pad did not convey any information related to self-motion. We favored these manipulations over transecting the infraorbital nerve on both sides to circumvent dual deficits of the whole face, which include impediment to eating (Jacquin and Zeigler, 1983). Four days after deafferentation, rats were re-exposed to the task. The effectiveness of the facial nerve lesion was assessed by the absence of vibrissa movement on the corresponding side (see Movie 2). The effectiveness of the infraorbital nerve lesion was assessed, after behavioral experiments were completed, by the absence of an evoked local field potential in the ventral posteromedial nucleus of the thalamus on electrical stimulation of the mystacial pad (see Fig. 5c). The recording site was labeled by an iontophoretic injection of Chicago Sky Blue (Sigma-Aldrich). Thereafter the rat was perfused, and brain tissue was processed for histology.

Cortical lesion

The vibrissa motor cortex was unilaterally or bilaterally lesioned by the application, over the pia mater, of a small crystal of silver nitrate, a strong cauterizing agent (Lavallée et al., 2005; centered 2 mm on the anteroposterior axis and 2 mm on the mediolateral axis with respect to the bregma). In case of unilateral lesion, the cortex contralateral to the tracked vibrissa was lesioned. The crystal was left in place for 5 min to allow diffusion of the chemical to the deep layers. Then the cortex was abundantly rinsed with saline and aspirated. At the end of the behavioral experiments, the rat was perfused, and brain tissue was cut at 60 µm on a freezing microtome. Sections were immunoreacted with a rabbit anti-NeuN antibody (Invitrogen) and an anti-rabbit antibody conjugated to Alexa Fluor 594 (Thermo-Fisher Scientific). Images of the cortical lesion were acquired using a slide scanner (Huron Digital Pathology).

Chemogenetic transient inactivation

Inhibitory designer receptors exclusively activated by designer drugs (DREADDs) were expressed in rubrofacial neurons via dual viral injections (100 nl each); adeno-associated virus (AAV)-hSyn-DIO-hM4D(Gi)-mCherry (catalog #44362, Addgene) was injected in the right parvocellular red nucleus and retrograde AAV-hSyn.Cre.WPRE.hGH (catalog #105553, Addgene) was injected in the lateral sector of the left facial nucleus, which contains the vibrissa motoneurons (Deschênes et al., 2016). To target injections in the facial nucleus, we first used microstimulation to elicit vibrissa deflection (Herfst

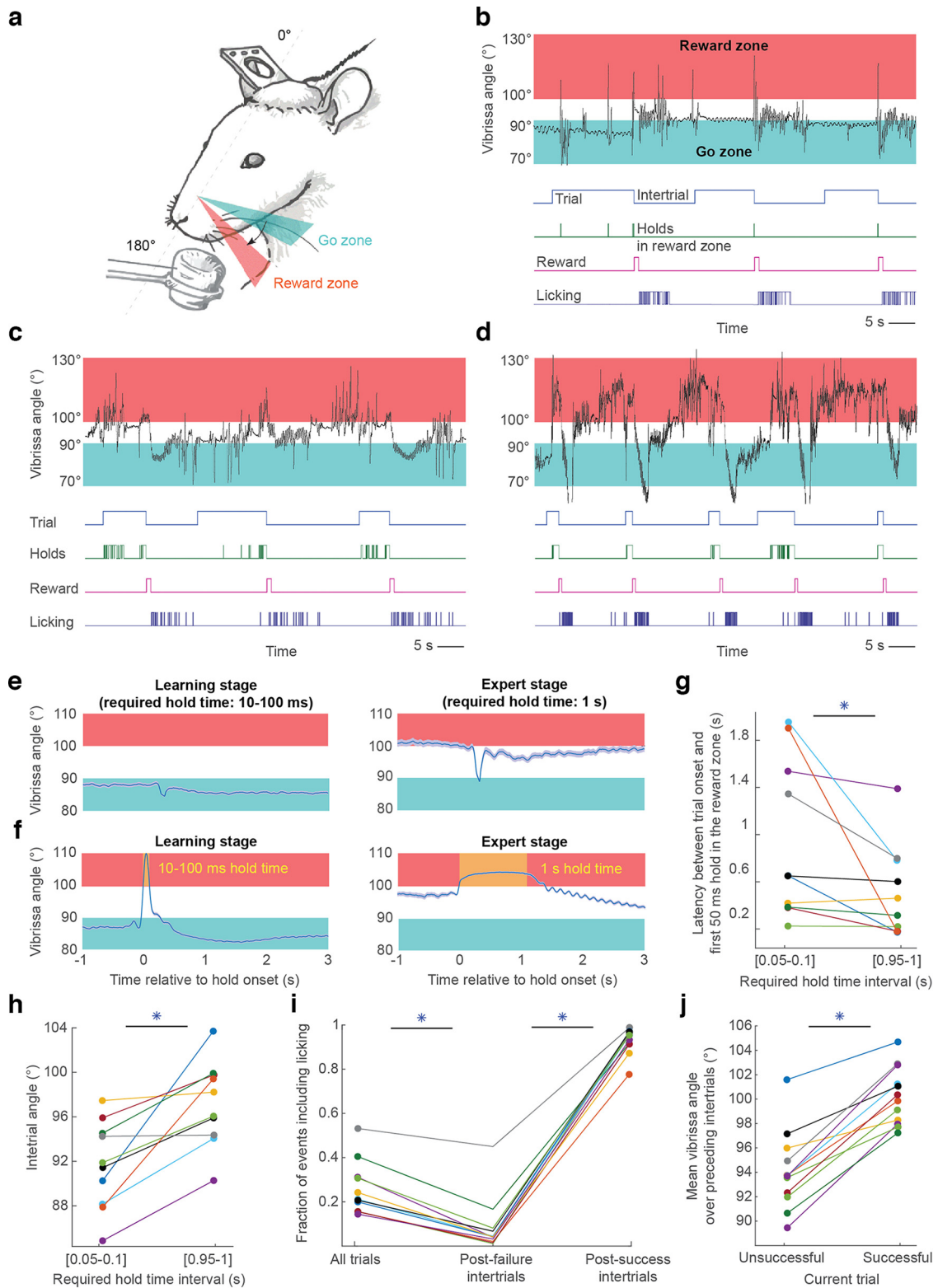


Figure 1. Intact animals can learn the vibrissa positioning task. **a**, Scheme of the vibrissa positioning task. Rats are trained to move their vibrissae from a retracted zone (Go zone) to a protracted zone (Reward zone) and maintain their vibrissae within the reward zone for a given duration (required hold time). The required hold time adaptively increases over training sessions. **b**, Sequence execution of the task by a naive rat (required hold time, 10 ms). **c**, Sequence execution of the task by a learning rat (required hold time, 400 ms). **d**, Sequence execution of the task by an expert rat (required hold time, 1 s). **e**, Mean vibrissa position at trial initiation over learning (mean \pm 95% confidence interval; data from a representative intact rat; left, 2323 trials; right, 542 trials). **f**, Mean vibrissa position over successful holds in the reward zone over learning (mean \pm 95% confidence interval; data from a representative rat; left, 1819 trials; right, 456 trials). **g**, Median latency between trial onset and first hold in the reward zone for at least 50 ms over learning (each color represents a specific rat; mixed-effect linear regression, $p = 0.016$). **h**, Mean vibrissa angle during intertrials over learning (each color represents a specific rat; mixed-effect linear regression, $p = 6.1 \times 10^{-6}$). **i**, Fraction of events which include licking, in intact expert rats (required hold time, 1 s; reward zone, 100–130°; each color represents a specific rat; mixed-effect logistic regressions, all trials vs postfailure intertrials, $p = 1.7 \times 10^{-21}$; postfailure intertrials vs postsuccess intertrials, $p = 4.4 \times 10^{-115}$). Licks occurring during trials and postfailure intertrials are false alarm licks. **j**, Relationship between vibrissa angle during intertrials

and Brecht, 2008). Thereafter, the virus was injected at the very same location. The red nucleus was located by stereotaxy (1 mm lateral to the midline, 5.5 mm behind the bregma, 6.5 mm below the dura).

After the viral injections, the craniotomies were covered with a silicone sealant (Kwik-Cast), and a head plate was fixed to the skull. Inactivation experiments were conducted at least 4 weeks after the viral injections.

To inactivate neurons expressing DREADD, clozapine *N*-oxide (CNO) dihydrochloride (Tocris Bioscience) was intraperitoneally injected (2 mg/kg) 1 h before the behavioral test. The exact same procedure was used for rats that did not express DREADD (SHAM group).

When all the behavioral sessions were completed, the animals were perfused, and brains were processed for histology. Images of the red nucleus and brainstem were acquired using a confocal microscope (Zeiss).

Data analysis

Statistical analyses. All data analyses were conducted under MATLAB (MathWorks). Figures for groups of animals (see Figs. 6c, 9e) are the result of pooled analyses, in which the contribution of each animal to the final measures is equivalent. All plus-minus (\pm) intervals, error bars, and shaded plot areas correspond to 95% confidence intervals, obtained through bootstrapping. The statistical tests used are linear and logistic mixed-effect models, chi-square tests, permutation tests, and likelihood-ratio tests.

Licking learning. To evaluate learning of the vibrissa positioning task, vibrissa data were analyzed only after rats had learned to lick reliably on water delivery, that is, after the reward could be tightly associated with a preceding action. The trial from which a rat is considered to lick reliably is defined as the first trial preceded by at least 80% licking occurrence in the first 2 s of the previous 250 postreward pauses. Reliable licking on reward delivery was achieved after 603 ± 191 rewards (mean \pm 95% CI).

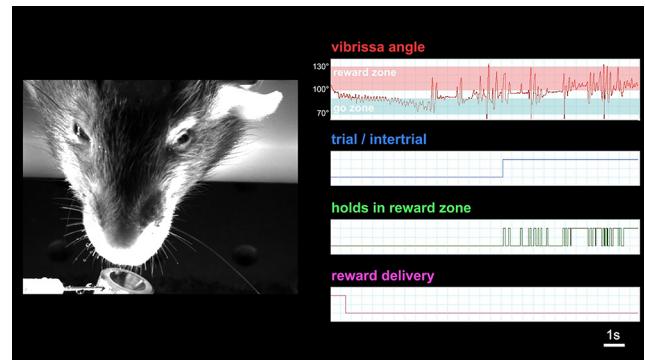
Task learning. As per our behavioral protocol, trial completion and reward delivery occurred as soon as rats maintained their vibrissa in the reward zone for the required hold time. As the required hold time increased over learning, a direct comparison of the vibrissa position over entire trials at different stages of learning is not possible. To compute the latency between trial onset and first hold in the reward zone of a duration of ≥ 50 ms, we excluded trials whose required hold time was lower than 50 ms. In contrast, periods between trials, that is, intertrials, are similar over learning; they all end as soon as the vibrissa reaches the go zone, provided that the intertrial pause has elapsed. Thus, vibrissa position during intertrials can be compared over learning. In analyses of intertrials, pauses following successful trials dedicated to licking were excluded from the analyses. For analyzing the evolution of the intertrial angle over learning, the angular mean of each intertrial was computed and retained as one observation.

Attempted trials. Attempted trials are trials during which the vibrissa was held in the reward zone for at least 50 ms continuously. At the expert level (required hold time, 1 s), empirical cumulative distributions of the maximum hold times in the reward zone and vibrissa angle density distribution were computed from attempted trials.

False alarm licks. These are licks that occur either during trials or during postfailure intertrials, that is, with no relation to water delivery. During any given trial, a false lick does not interrupt the ongoing trial and, therefore, does not imply failure at the trial in question. The fraction of events including licking was compared across the three types of

←

and success in subsequent trials in expert rats (required hold time, 1 s; reward zone, 100–130°; each color represents a specific rat; mixed-effect logistic regression, $p = 1.5 \times 10^{-26}$). * $p < 0.05$.



Movie 1. Execution of the vibrissa positioning task by an intact expert rat. [View online]



Movie 2. Lesion of the facial motor nerve results in motor paralysis. [View online]

events of our task—trials, postsuccess intertrials, and postfailure intertrials. The onset of these three events is accompanied by a specific 300-ms-long audio cue. To control for the possibility that any of these three audio cues may induce licking via a reflex response, we computed how often licking occurred only from 2 to 3 s after any of the cues was played (if an event was lasting < 3 s, it was discarded; Fig. 1i).

Influence of success history on current performance. We investigated the relationship between past success and current performance by using mixed-effect logistic regression models on multiple series of consecutive trials during each of which rats held their vibrissa in the reward zone for at least 400 ms. Each series contained at least 10 trials. The models used past successes as predictors and current success as the response variable. Starting with a null model that included only the intercept and subject-related random effects, we iteratively added one additional trial farther back in the past to the list of predictors in each subsequent iteration. We compared the nested and full models, containing $n-1$ and n trials in the past, at each iteration using a likelihood-ratio test. The algorithm was interrupted as soon as adding an additional trial farther back in the past no longer significantly improved the model.

Recovery after deafferentation. The session from which rats were considered to have recovered from deafferentation was the first of the three consecutive sessions following deafferentation whose pooled success rate was not statistically lower than the pooled success rate of the last three sessions preceding deafferentation (chi-square test, $p > 0.05$). All subsequent analyses aimed at comparing steady-state execution before and after deafferentation were conducted with the postrecovery data.

Spectral analyses. Spectral analyses were conducted using multitaper estimates (Kleinfeld and Mitra, 2014) as implemented in the Chronux MATLAB toolbox (Bokil et al., 2010). Following a procedure previously described (Hill et al., 2011), whisking bouts were detected using spectrograms, and whisking parameters, that is, set point, amplitude and phase, were extracted using the Hilbert transform (Hill et al., 2011; Moore et al., 2013).

Results

The vibrissa positioning task

Head-restrained rats were trained to move their left C1 vibrissa (Brecht et al., 1997) from a retracted position (70–90° with respect to the anteroposterior axis), denoted the go zone, to a protracted position (100–130°), denoted the reward zone (Fig. 1*a–d*; Movie 1). Once rats self-initiated trials by positioning their vibrissa in the go zone, they were allowed a maximum of 10 s to reach and hold their vibrissa within the reward zone for a given required hold time. The required hold time adaptively increased over learning, from 10 ms initially to 1 s at the expert level (and for one animal of our 17 expert rats, up to 2 s). Once rats reached the expert level, the hold time was fixed, and the effect of experimental manipulations was assessed. At no point in the training could the rats use touch or vision to estimate vibrissa position.

Intact rats can learn the vibrissa positioning task

Naive rats tended to maintain their vibrissa within the go zone and, given the short initial required hold time (10 ms), could succeed through brief forward twitches into the reward zone (Fig. 1*b,e,f*). Over learning (3760 ± 1236 trials on average to reach the expert criterion for 10 intact rats; Fig. 2), rats reached and maintained their vibrissa in the reward zone more swiftly following trial onset (Fig. 1*g*; mixed-effect linear regression, $p < 0.05$). They displayed an increasing trend to protract, including during intertrials (Fig. 1*c–e*; 1*h*; mixed-effect linear regression, $p < 0.01$). Ultimately, contrary to naive rats, experts started most trials via backward twitches toward the go zone (Fig. 1*d–e*; Movie 1).

The increased protraction expert rats displayed during intertrials may either be the consequence of an effective strategy to succeed or of the incapacity to distinguish between trials and intertrials. We invalidated the latter hypothesis by showing that the likelihood of false alarm licks is higher during trials during postfailure intertrials (Fig. 1*i*; mixed-effect logistic regression, $p < 0.01$), a probable mark of the higher expectation of receiving a reward once trials have started. Interestingly, the larger the vibrissa angle during an intertrial, the higher the likelihood of succeeding in the subsequent trial (Fig. 1*j*; mixed-effect linear regression, $p < 0.01$). This observation may be used to shed light on the strategy of the rats during the task; do they dynamically rely on recent success history to maintain their vibrissa in locations that were proven successful? To test this possibility, we ran logistic regression models predicting success at any given trial, based on the success history of previous trials. Importantly, only series of consecutive trials during which rats were actively protracting (each trial containing at least one hold of at least 400 ms in the reward zone) were included to rule out dependencies due to within-session fluctuations in, for example, motivation. Considering up to three trials in the past significantly improves the prediction of success on the present trial (likelihood ratio test, $p < 0.05$). This clustering of successes in time suggests angular adjustments within and close to the reward zone that deploy and are maintained within series of consecutive trials.

We next considered the extent of adaptability of the motor control for this task. We submitted expert rats to two adaptation protocols, with all experiments conducted at the expert required hold time criterion (1 s).

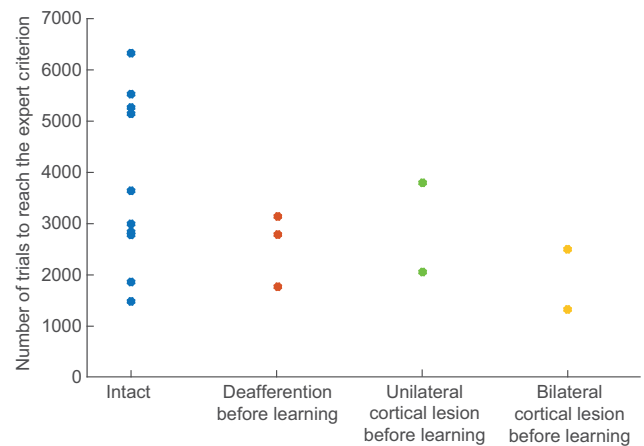


Figure 2. Number of trials to reach the expert criterion. Each point relates to a specific animal.

Adaptation protocol 1

With the first adaptation protocol, the upper limit of the reward zone, initially 130°, was progressively lowered as a function of the performance of the animal, down to 110° (Fig. 3*a*). We evaluated whether rats became better at succeeding with a 100–110° reward zone criterion when they had de facto been trained at 100–110° compared with when they had de facto been trained at 100–130°. In case of effective adaptation, one would expect a higher success rate at 100–110° when animals were de facto trained at this reward zone. Yet, this comparison requires an important control to be unbiased. We reprocessed the trials de facto collected within the 100–110° criterion to trim those that would have been successful under the 100–130° criterion because, during the actual task, success interrupted any ongoing trial. The period of the trials posterior to the trimming time, that is, posterior to the end of the first successful hold at 100–130°, was further disregarded from the analysis. Then, we determined the success rate at 100–110° for these trials. We also reprocessed the trials de facto trained at 100–130° to determine what the success rate would have been under the 100–110° criterion. Both these simulated success rates at 100–110° can then be unbiasedly compared. A side effect of our control procedure is that it reduces the amount of vibrissa data available for the simulations, which decreases the simulated success rates and underestimates the performance of the animals by inflating false negatives. Yet, this conservative procedure is essential and allows for statistical comparisons. All intact expert rats displayed a higher success rate at the 100–110° criterion when they were de facto trained at 100–110° rather than at 100–130° (Fig. 3*b*). This finding is consistent with effective adaptation to a narrow reward zone.

Adaptation protocol 2

Once rats reached a 100–110° reward zone through the first adaptation protocol, they were exposed to a second adaptation protocol whereby both upper and lower limits of the reward zone were moved across successive sessions in such a way that the width of the reward zone remained equal to 10°. Specifically, each expert rat was alternatively exposed to two reward zones (one per session), 100–110° and 105–115° (Fig. 4*a*). We compared the success rate for trials actually trained at 105–115° with the simulated success rate for the same trials if the animals had been trained at 100–110°. Similarly, we compared the success

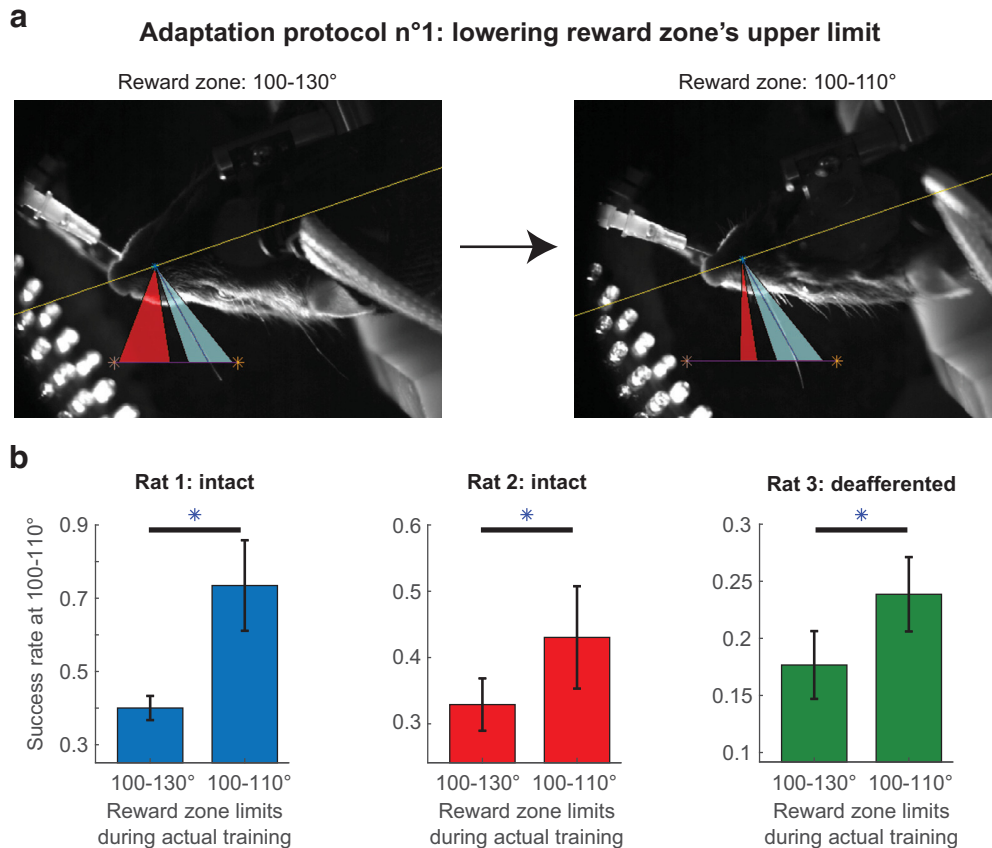


Figure 3. First adaptation protocol. **a**, Scheme of the first adaptation protocol. **b**, Task performance for three expert rats (each color represents a specific rat; chi-square tests, rat 1, $p = 4.0 \times 10^{-6}$; rat 2, $p = 0.019$; rat 3, $p = 0.0060$). $*p < 0.05$.

rate for trials actually trained at 100–110° with the simulated success rate for the same trials if the rats had been trained at 105–115°. This analysis controls for the possibility that rats merely progressively protracted (or retracted) their vibrissa to succeed in trials independently of the reward zone, which would be a way to succeed with either reward zone without adapting. One of the two intact expert rats subjected to this protocol successfully adapted to both reward zones, whereas the other gave up when exposed to 105–115° as shown by a relative retraction of its vibrissa position when exposed to this more protracted reward zone (Fig. 4*b,c*).

In summary, the vibrissa positioning task exhibits fine voluntary motor control of the vibrissa position.

Vibrissa sensory feedback is neither required to learn nor to execute the task

Do rats require sensory feedback to finely move their vibrissae? This is physiologically plausible as vibrissa reafferent signals, encoded by mechanoreceptor afferents (Wallach et al., 2016; Severson et al., 2017; Severson et al., 2019), are present in the rodent brainstem (Zucker and Welker, 1969; Moore et al., 2015*b*; Wallach et al., 2016), thalamus (Yu et al., 2006; Moore et al., 2015*b*; Urbain et al., 2015; Gutnisky et al., 2017), sensory cortex (Fee et al., 1997; Curtis and Kleinfeld, 2009; Ranganathan et al., 2018; Cheung et al., 2019; Isett and Feldman, 2020), motor cortex (Kleinfeld et al., 2002), and cerebellum (O'Connor et al., 2002; Chen et al., 2016).

To test the requirement of sensory feedback to learn the task, we deafferented rats before their first training session, taking

advantage of the separation of the vibrissa sensory and motor nerves (Fee et al., 1997; Fig. 5*a–c*; Movie 2). Deafferented rats displayed the same signs of learning as intact rats and reached the expert level with quasi-maximum performance to the task (Fig. 5*d–g*; for three rats).

To test the requirement of sensory feedback to execute the task once learned, we deafferented expert rats. All deafferented rats regained their prelesion success rate within a few experimental sessions (three rats after seven to nine sessions; Fig. 6*a*). Deafferentation did not change the vibrissa mean angle during trials (Fig. 6*b*; mixed-effect linear regression, $p = 0.34$), nor change the across-trial variability during the expert holds (Fig. 6*c,d*; permutation test, $p = 0.58$). Finally, one expert rat that was deafferented after learning was exposed to the two adaptation protocols previously described to which it adapted successfully (Figs. 3*b*, 4*b,c*).

All told, the vibrissa sensory feedback is neither required for learning nor for executing the vibrissa positioning task. This implies that rats can finely control their vibrissa position via an open-loop controller.

Motor cortex is neither required to learn nor to execute the task

As the vibrissa position can be decoded from the vibrissa motor cortex (Kleinfeld et al., 2002; Hill et al., 2011; Friedman et al., 2012; Sreenivasan et al., 2016; Ebbesen et al., 2017) both in the presence and in the absence of sensory feedback (Hill et al., 2011), we tested the requirement of motor cortex in the task, before and after deafferentation. We ablated the motor cortex of naive rats (Fig. 7*a*) and initiated training

a Adaptation protocol n°2: moving upper and lower limits of a 10°-wide reward zone

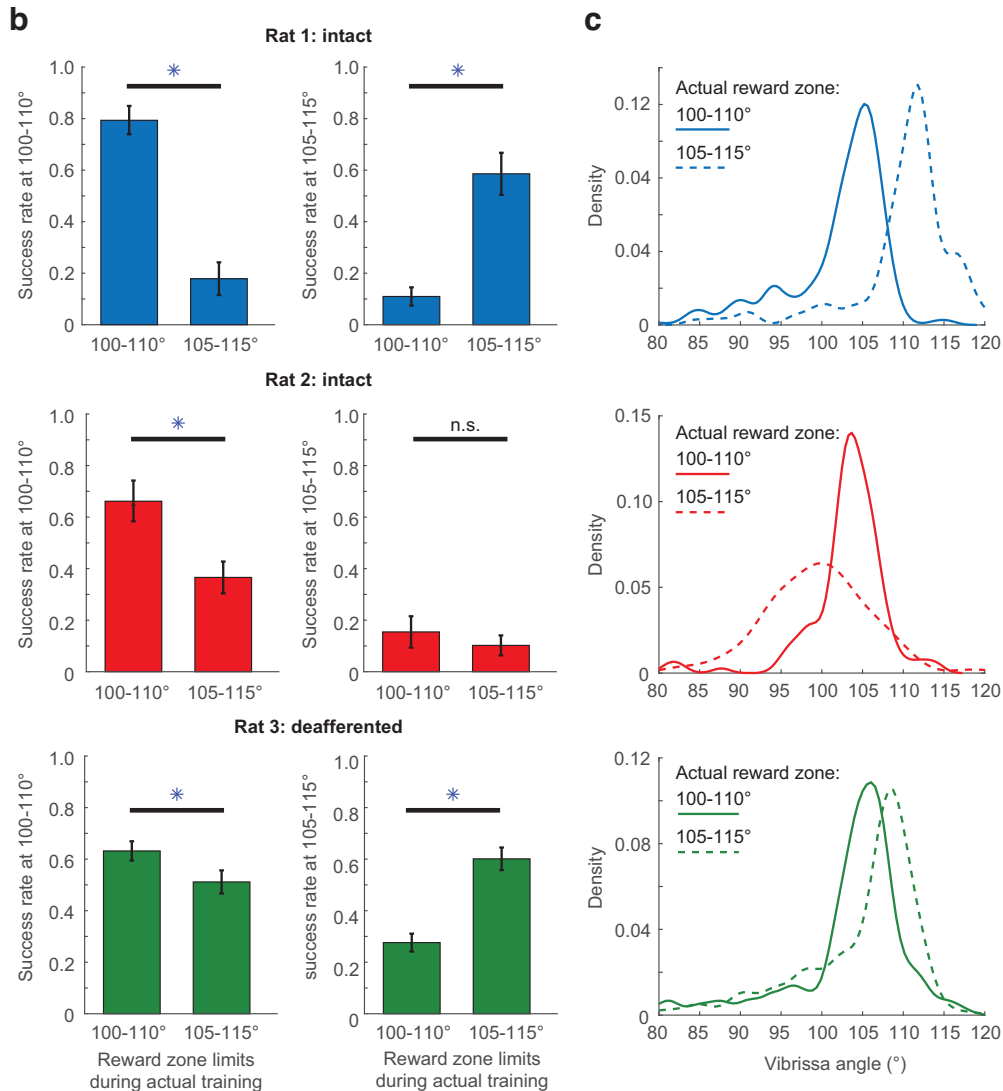
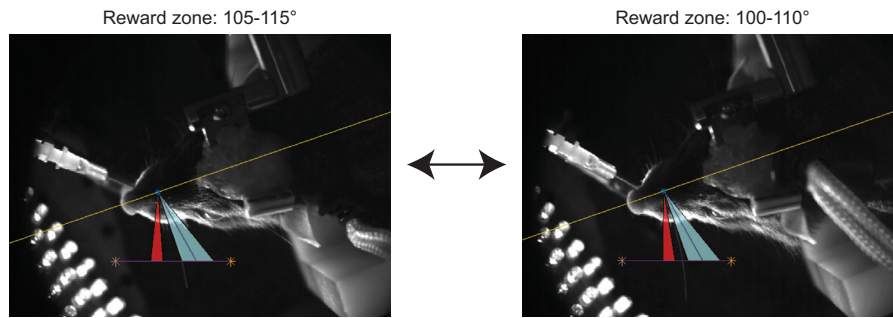


Figure 4. Second adaptation protocol. **a**, Scheme of the second adaptation protocol. **b**, Task performance for the same three expert rats as in Figure 3 [color/rat associations are the same as in Fig. 3; chi-square tests, rat 1, $p = 8.1 \times 10^{-18}$ (left), 3.0×10^{-26} (right); rat 2, $p = 3.5 \times 10^{-9}$ (left), 0.14 (right); rat 3, $p = 5.4 \times 10^{-5}$ (left), 8.8×10^{-28} (right)]. **c**, Density distribution of the mean vibrissa position over the last second of each trial (color/rat associations are the same as in Fig. 4b; rat 1, 100–110°, 341 trials; 105–115°, 140 trials; rat 2, 100–110°, 136 trials; 105–115°, 235 trials; rat 3, 100–110°, 641 trials; 105–115°, 479 trials). * $p < 0.05$; n.s. denotes $p > 0.05$.

to the task. Decorticated rats displayed the same signs of learning as intact rats and reached the expert level (Figs. 7b–d, 8a; for four rats), with comparable execution reliability as intact rats (Figs. 6d, 8d). We conclude that the motor cortex is neither required for learning nor for executing the vibrissa positioning task in the presence of sensory feedback.

Absent motor cortex, sensory feedback is required for vibrissa stability

To test the requirement of vibrissa motor cortex in the absence of sensory feedback, we deafferented our decorticated expert rats. All deafferented decorticated rats recovered their pre-deafferentation success rate (4 rats after 7–11 sessions; Fig. 8a). Yet, surprisingly, deafferentation of decorticated rats led to a

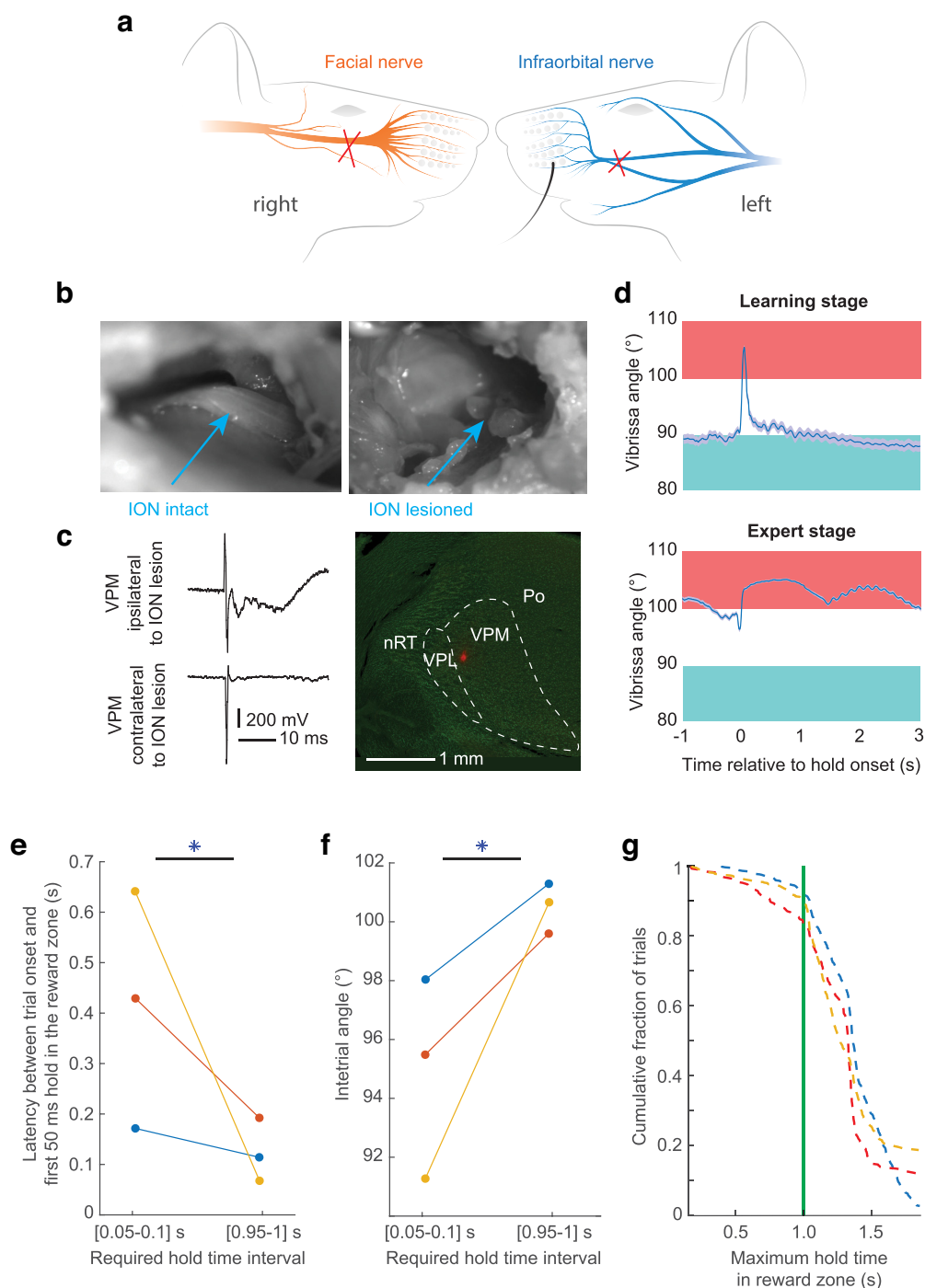


Figure 5. Sensory feedback is not required to learn the task. **a**, Scheme of the deafferentation procedure. The infraorbital nerve is transected on the side of the tracked vibrissa; the buccal and marginal branches of the facial nerve are transected on the opposite side. **b**, Pictures of the infraorbital nerve, before and after transection (data from a representative rat). **c**, Left, *Post hoc* assessment of the effectiveness of the infraorbital nerve lesion through bilateral local field potential recording in the vibrissa ventral posteromedial nucleus (VPM) of the thalamus, during electrical stimulation of pad muscles (data from a representative rat). Right, Fluorescent (Chicago Sky Blue) red spot in the VPM, iontophoretically injected at the end of the local field potential recording contralaterally to the infraorbital lesion. VPL, Ventral posterolateral nucleus of the thalamus; PO, posterior nucleus of the thalamus; nRT, reticular nucleus of the thalamus. **d**, Mean vibrissa position over successful holds in the reward zone over learning (mean \pm 95% confidence interval; data from a representative rat; top, 312 trials; bottom, 670 trials). **e**, Median latency between trial onset and first hold in the reward zone for at least 50 ms over learning (each color represents a specific rat; mixed-effect linear regression, $p = 4.1 \times 10^{-15}$). **f**, Mean vibrissa angle during intertrials over learning (each color represents a specific rat; mixed-effect linear regression, $p = 2.4 \times 10^{-4}$). **g**, Empirical cumulative distribution of the maximum hold times in the reward zone across trials in three expert rats deafferented before learning (each color represents a specific rat; required hold time, 1 s; reward zone, 100–130°). * $p < 0.05$.

permanent motor precision deficit that did not occur in rats with intact cortex; the variability of the vibrissa angle increased across trials (Fig. 8*b*; permutation test, $p < 0.01$), including across successful expert holds (Fig. 8*c,d*; permutation test, $p < 0.01$).

We conclude that in the absence of motor cortex and sensory feedback, rats are still able to perform the task, but they perform it with diminished motor reliability. These results indicate that in the absence of motor cortex, sensory feedback plays a noncompensable role in the ability to stabilize motor output.

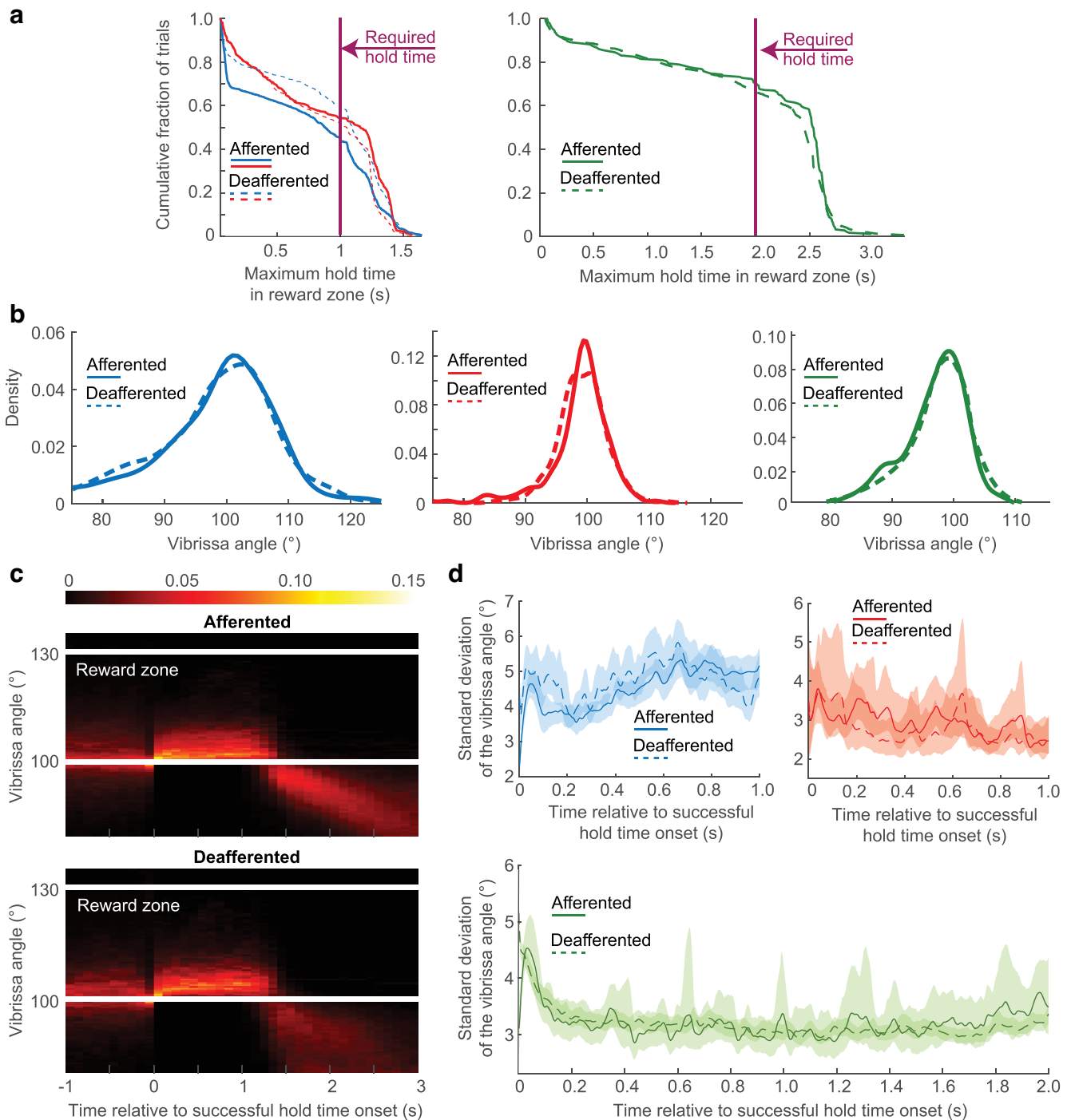


Figure 6. Sensory feedback is not required to execute the task. **a**, Empirical cumulative distribution of the maximum hold times in the reward zone across trials, before and after deafferentation, in three expert rats [each color represents a specific rat; required hold time, 1 s (left) or 2 s (right); reward zone, 100–130°]. **b**, Vibrissa angle distribution over trials, before and after deafferentation, for three expert rats [color/rat associations are the same as in Fig. 6a; required hold time, 1 s (left and middle) or 2 s (right); reward zone, 100–130°; rat 1 (blue) afferented, 994 trials; deafferented, 442 trials; rat 2 (red) afferented, 462 trials; deafferented, 265 trials; rat 3 (green) afferented, 809 trials; deafferented, 579 trials]. **c**, Histograms of the vibrissa position during successful holds, before and after deafferentation, as the pooled mean across two expert rats (required hold time, 1 s; reward zone, 100–130°; top, 688 trials; bottom, 398 trials). The color bar denotes the probability of presence. **d**, Angular SD across successful holds, before and after deafferentation, for three expert rats [$SD \pm 95\%$ confidence interval; color/rat associations are the same as in Fig. 6a; required hold time, 1 s (top) or 2 s (bottom); reward zone, 100–130°; permutation test, $p = 0.58$; rat 1 (blue) afferented, 437 trials; deafferented, 262 trials; rat 2 (red) afferented, 251 trials; deafferented, 136 trials; rat 3 (green) afferented, 569 trials; deafferented, 388 trials].

Inactivation of the rubrofacial pathway disrupts performance

Amid the numerous premotor nuclei controlling vibrissa motoneurons (Isokawa-Akesson and Komisaruk, 1987; Hattox et al., 2002; Takatoh et al., 2013; Sreenivasan et al., 2015; McElvain et al., 2018), the parvocellular part of the red nucleus is of particular

interest. First, it receives inputs from motor cortex and cerebellum (Daniel et al., 1987; Hattox et al., 2002; Pacheco-Calderón et al., 2012), which both anticipate vibrissa position (Hill et al., 2011; Chen et al., 2016). Second, it has access to vibrissa sensory information via direct projections from the trigeminal sensory nuclei (Godefroy et al., 1998; Elbaz et al., 2022). Thus, inputs

to the red nucleus make it a potential integrator of efferent and reafferent signals.

We examined the involvement of the rubrofacial pathway by expressing an inhibitory DREADD (Zhu and Roth, 2014) in rubral neurons that project to the facial motor nucleus, which drives movement of the vibrissae (Figs. 9*a*, 10). This expression allowed for the conditional inactivation of rubrofacial neurons throughout the entire duration of test sessions, following intraperitoneal injection of CNO. To account for potential endogenous effects of CNO (Gomez et al., 2017; Mahler and Aston-Jones, 2018; Manvich et al., 2018), the effects of CNO were compared between expert rats expressing DREADD and expert rats not expressing DREADD (three subjects in each group). Inactivation of the red nucleus decreased the proportion of attempted trials (Fig. 9*b*; mixed-effect logistic regression, interaction effect DREADD:CNO, $p < 0.01$) and increased the latency of attempts (Fig. 9*c*; mixed-effect logistic regression, interaction effect DREADD:CNO, $p < 0.01$). It dramatically impaired the ability of rats to maintain their vibrissa in the reward zone (Fig. 9*d*; mixed-effect logistic regression on success rates, interaction effect DREADD:CNO, $p < 0.01$). The vibrissa position during trials appeared much more retracted under rubrofacial inactivation (Fig. 9*e*; mixed-effect linear regression, interaction effect DREADD:CNO, $p < 0.01$), and its variability was increased (permutation test, $p < 0.05$). This higher retraction was also observed during rhythmic, whisking movements of the vibrissa (Welker, 1964; Hill et al., 2011; Fig. 9*f*; mixed-effect linear regression on whisking set point, interaction effect DREADD:CNO, $p < 0.05$). This suggests the existence of a regulatory mechanism for set point independent of whisking, an idea consistent with the persistence of set point control after lesion or inactivation of the whisking oscillator (Kleinfeld et al., 2014; Takatoh et al., 2022).

These results indicate that the rubrofacial pathway is critically involved in the initiation and execution of the vibrissa positioning task. They further suggest the involvement of the red nucleus as part of the motor controller.

Discussion

We aimed to identify the mechanisms whereby rats can keep track of the position of their moving vibrissae (Kleinfeld and Deschênes, 2011; Cheung et al., 2019). Toward this goal, we trained rats to perform a vibrissa positioning task without the possibility of contact. Our experimental model allowed us to disentangle internal (efference copy) components from external (reafference based) ones during the execution of a fine motor

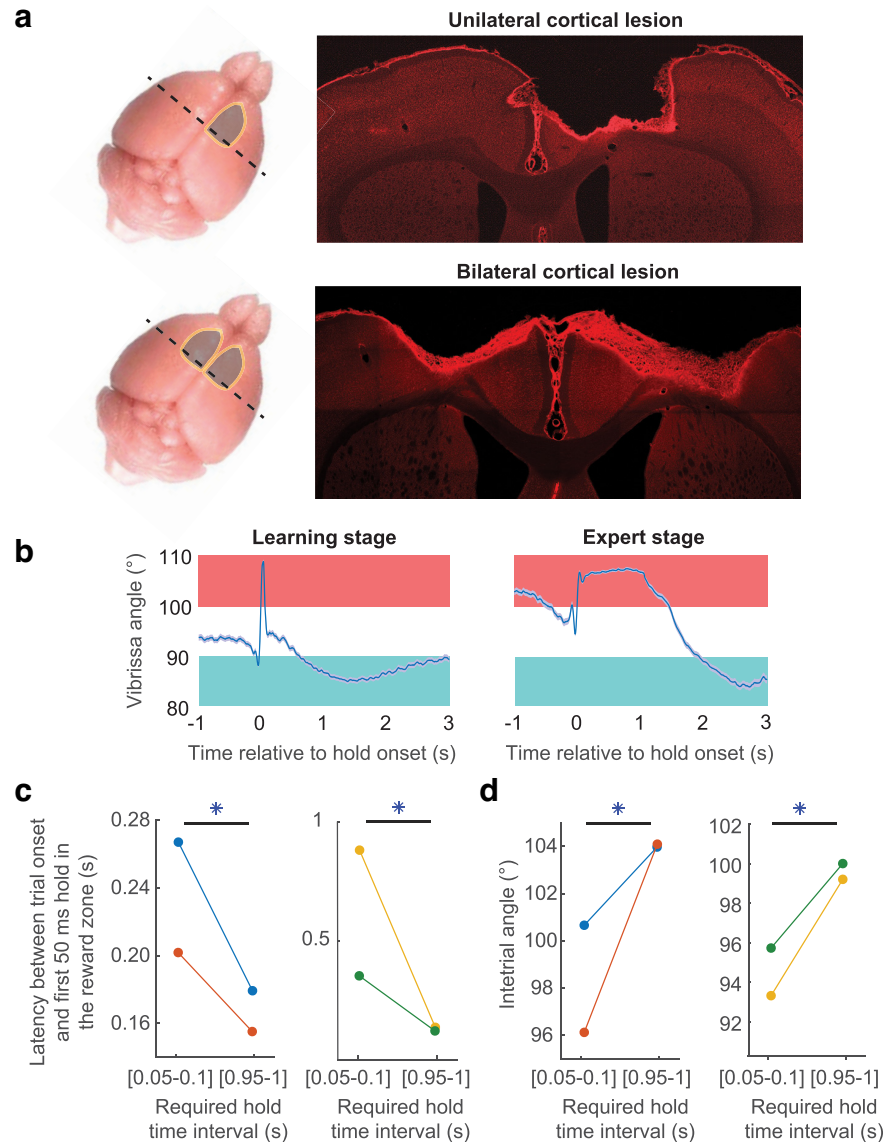


Figure 7. Motor cortex is not required to learn the task. **a**, Scheme and fluorescent microscopy image of unilateral and bilateral motor cortical lesions (coronal sections). The tissue was counterstained with a generic neuronal biomarker (anti-NeuN antibodies). **b**, Mean vibrissa position over successful holds in the reward zone over learning (mean \pm 95% confidence interval; data from a representative rat with bilateral cortical lesion; left, 998 trials; right, 588 trials). **c**, Median latency between trial onset and first hold in the reward zone for at least 50 ms over learning (each color represents a specific rat (left, unilateral cortical lesion; right, bilateral cortical lesion; mixed-effect linear regression, left, $p = 0.023$; right, $p = 0.037$). **d**, Mean vibrissa angle during intertrials over learning (each color represents a specific rat; left, unilateral cortical lesion; right, bilateral cortical lesion; mixed-effect linear regression, left, $p = 3.8 \times 10^{-4}$; right, $p = 0.036$). * $p < 0.05$.

action. We accomplished this by exploiting an anatomic advantage of the vibrissa system, which enables vibrissa afference to be manipulated independently of the motor drive (Fee et al., 1997), and the specificity of our touch-free task, for which deafferentation of animals is strictly akin to abolishing peripheral reafference. Three conclusions emerged from our findings. First, rats can reliably and accurately control the position of their vibrissa independently of touch (Fig. 1) and, critically, after deafferentation (Figs. 5, 6). These results imply the existence of an open-loop internal representation for the vibrissa position in the nervous system, precisely mapped with corresponding motor commands. Second, rats whose motor cortex was ablated learned the task (Fig. 7). Deafferentation decreased the reliability of motor control in decorticated rats but not in rats with an

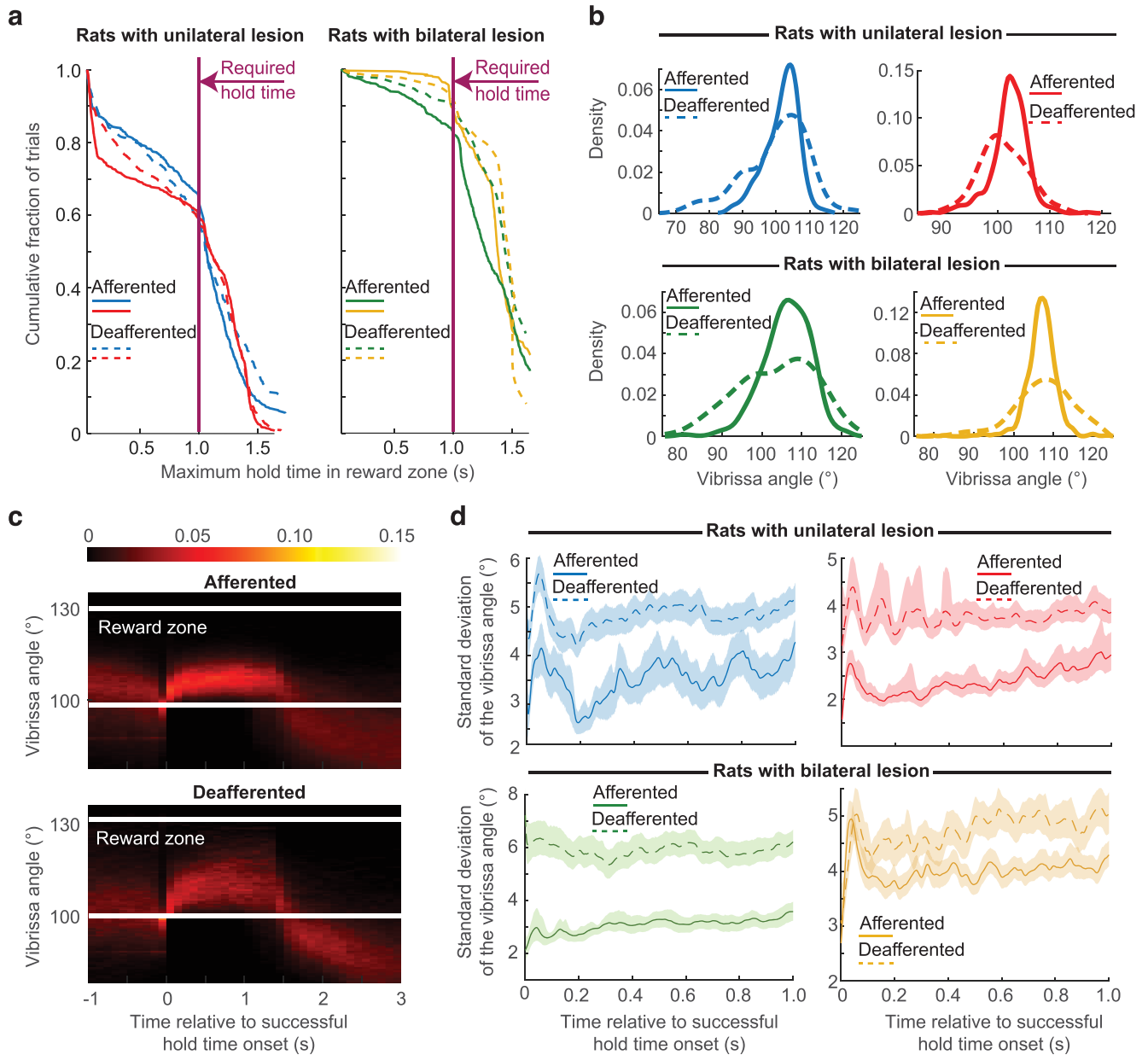


Figure 8. Motor cortex is required for motor stability in case of deafferentation. **a**, Empirical cumulative distribution of the maximum hold times in the reward zone across trials in four decorticated rats, before and after deafferentation (each color represents a specific rat; required hold time, 1 s; reward zone, 100–130°). **b**, Vibrissa angle distribution over trials, before and after deafferentation, for four expert rats with a cortical lesion [color/rat associations are the same as in Fig. 8a; required hold time, 1 s; reward zone, 100–130°; rat 1 (blue), afferented, 270 trials; deafferented, 710 trials; rat 2 (red), afferented, 584 trials; deafferented, 347 trials; rat 3 (green), afferented, 650 trials; deafferented, 275 trials; rat 4 (yellow), afferented, 661 trials; deafferented, 414 trials]. **c**, Histograms of the vibrissa position during 1 s successful holds in bilaterally decorticated rats, before and after deafferentation, as the pooled mean across two expert rats (required hold time, 1 s; reward zone, 100–130°; top, 1121 trials; bottom, 620 trials). The color bar denotes the probability of presence. **d**, Angular SD across 1 s successful holds, before and after deafferentation, for four expert rats with a cortical lesion [SD ± 95% confidence interval; color/rat associations are the same as in Fig. 8a; required hold time, 1 s; reward zone, 100–130°; permutation test, $p = 0.008$; rat 1 (blue), afferented, 173 trials; deafferented, 419 trials; rat 2 (red), afferented, 356 trials; deafferented, 212 trials; rat 3 (green), afferented, 533 trials; deafferented, 247 trials; rat 4 (yellow), afferented, 588 trials; deafferented, 373 trials].

intact brain (Fig. 8). This implies that reafferent signals and motor cortex are interchangeably required for stabilizing motor output. Finally, inactivation of rubrofacial neurons drastically impeded the performance of the rats (Fig. 9). This suggests that the red nucleus is the locus or at least a relay of the motor controller.

Contrary to permanent lesion of motor cortex or peripheral afferents, transient inactivation of rubrofacial neurons significantly impaired the success rate of the task. Two reasons may contribute to explaining this difference in effect. First, previous reports demonstrated that transient inactivation of a given brain

region can cause deficits that lesion of even the same brain region does not cause (Otchy et al., 2015; Wolff and Ölveczky, 2018; Vaidya et al., 2019). This is understandable because a lesion assesses requirement given that compensatory mechanisms can be at play, whereas a transient manipulation is most likely to test normal physiological involvement in the absence of compensatory mechanisms (but see Fetsch et al., 2018, demonstrating fast compensatory mechanisms unfolding in the space of single behavioral sessions). Second, inactivating the red nucleus is akin to concomitantly disrupting both cortical and cerebellar inputs conveyed through the red nucleus (Pacheco-Calderón et al.,

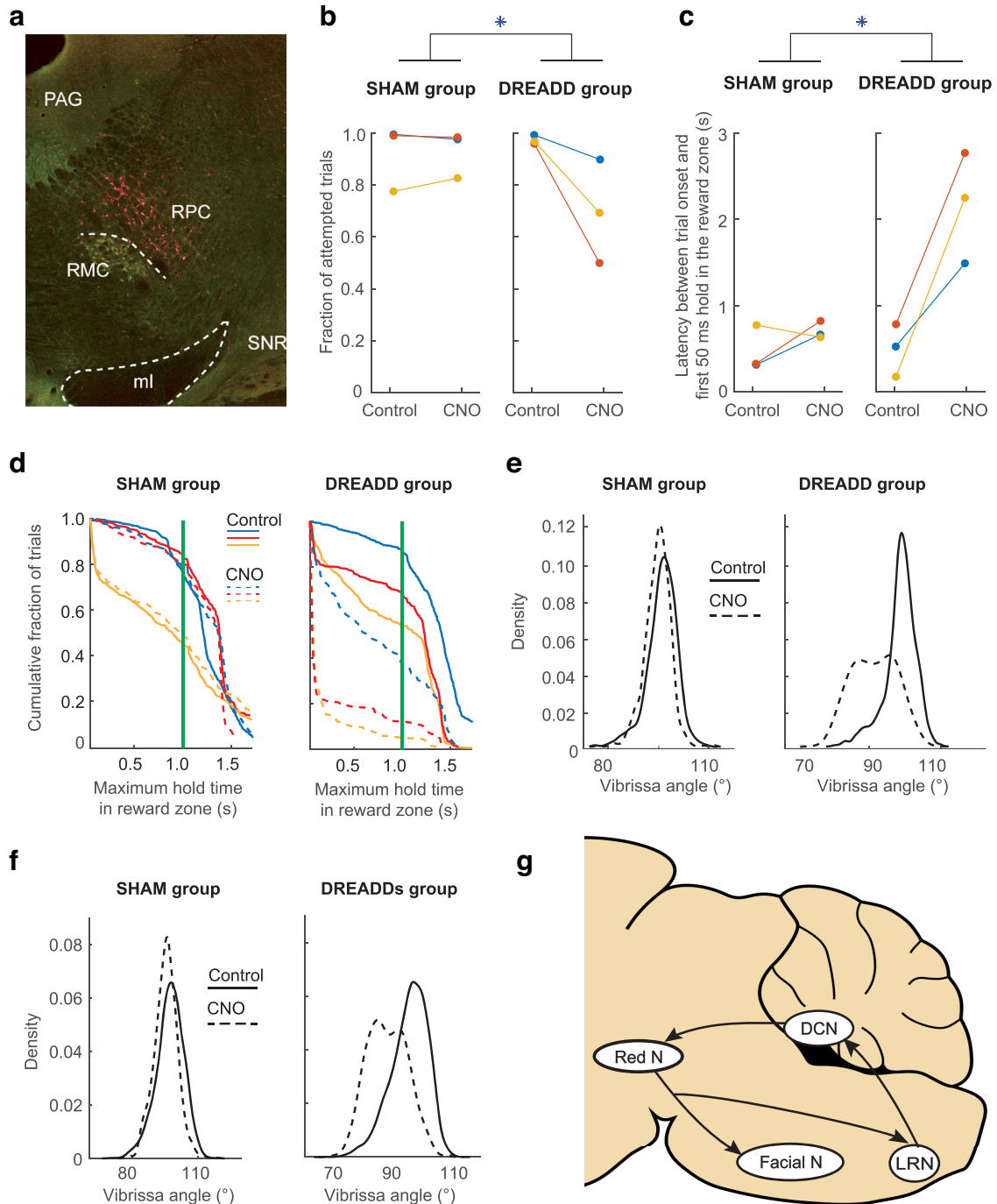


Figure 9. Inactivation of the rubrofacial pathway disrupts performance. **a**, Fluorescent microscopy image of the parvocellular red nucleus (coronal section), whose neurons express an inhibitory DREADD and a red fluorescent protein. ML, Medial lemniscus; PAG, periaqueductal gray; RMC, red magnocellular nucleus; RPC, red parvocellular nucleus; SNR, substantia nigra pars reticulata. **b**, Fraction of attempted trials, in DREADD and SHAM groups, before and after CNO administration. Each group includes three expert animals (each color represents a specific rat; required hold time, 1 s; reward zone, 100–130°; mixed-effect logistic regression, $p = 0.0032$). **c**, Median latency between trial onset and first hold in the reward zone for at least 50 ms, in DREADD and SHAM groups, before and after CNO administration. Each group includes three expert animals (each color represents a specific rat; required hold time, 1 s; reward zone, 100–130°; mixed-effect linear regression, $p = 0.0029$). **d**, Empirical cumulative distribution of the maximum hold times in the reward zone across trials in DREADD and SHAM groups, before and after CNO administration. Each group includes three expert animals (each color represents a specific rat; required hold time, 1 s; reward zone, 100–130°; mixed-effect logistic regression on success rates, interaction effect DREADD:CNO, $p = 1.1 \times 10^{-9}$). **e**, Vibrissa angle distribution over trials excluding whisking, in DREADD and SHAM groups, before and after CNO administration, as the pooled mean across rats. Each group includes three expert animals (required hold time, 1 s; reward zone, 100–130°; mixed-effect linear regression interaction effect DREADD:CNO, $p = 0.0091$; left, no CNO, 1698 trials; CNO, 877 trials; right, no CNO, 1703 trials; CNO, 699 trials). **f**, Vibrissa angle distribution over trials during whisking, in DREADD and SHAM groups, before and after CNO administration, as the pooled mean across rats. Each group includes three expert animals (required hold time, 1 s; reward zone, 100–130°; mixed-effect linear regression on whisking set point, interaction effect DREADD:CNO, $p = 0.039$; left, no CNO, 1903 whisking fragments; CNO, 911 whisking fragments; right, no CNO, 2361 whisking fragments; CNO, 1980 whisking fragments). **g**, Hypothetical circuit diagram of inputs and outputs of rubrofacial neurons. DCN, Deep cerebellar nuclei; Facial N, facial nucleus; LRN, lateral reticular nucleus; Red N, red nucleus. * $p < 0.05$.

Rubro-facial collaterals

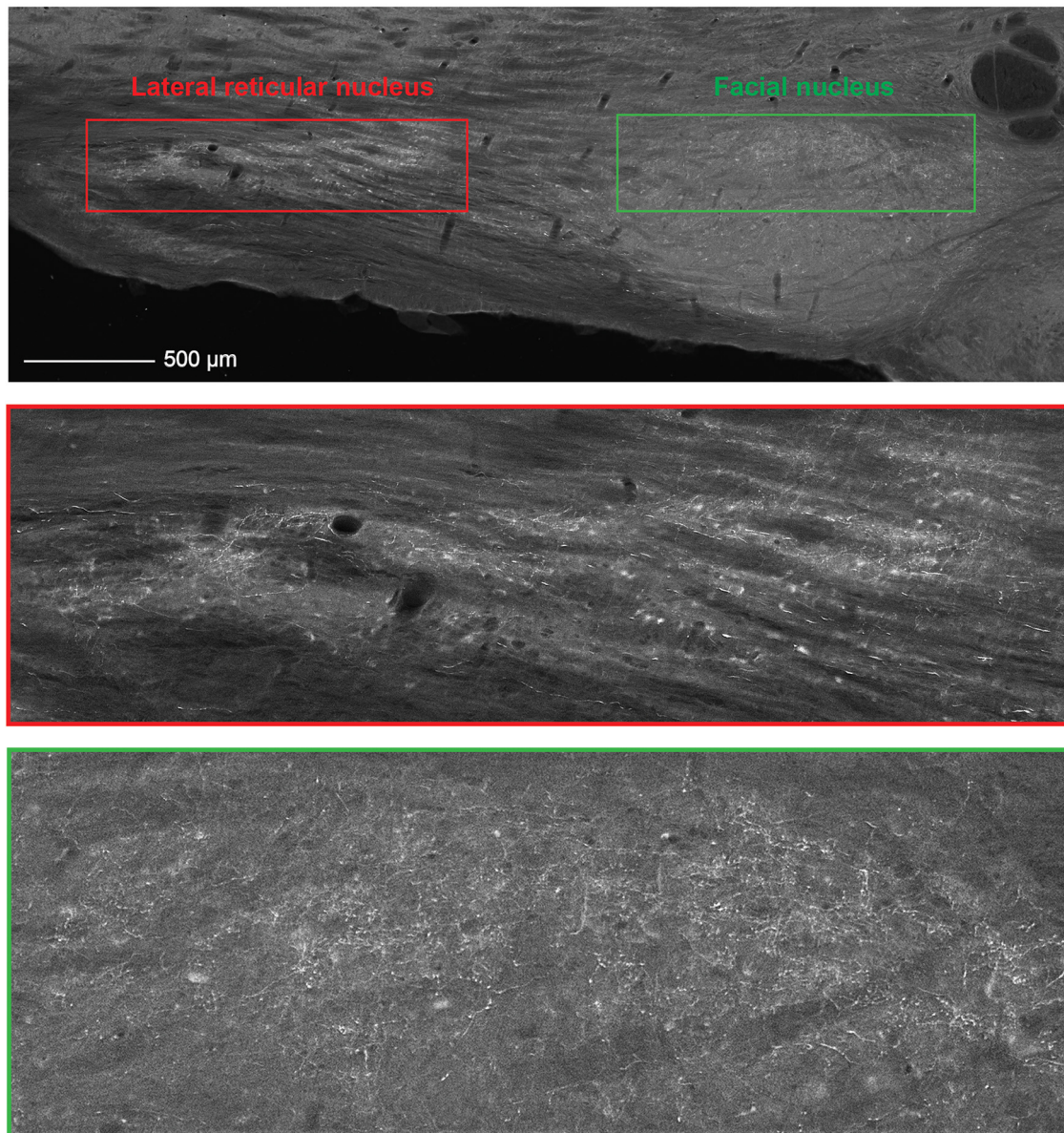


Figure 10. Rubrofacial collaterals. Axonal collaterals of rubrofacial neurons revealed by fluorescent microscopy (sagittal section; data from a representative rat). The labeled neurons coexpress a red fluorescent protein and an inhibitory DREADD.

2012), which our lesions do not reproduce. Thus, our results are consistent with at least partial dependence of cortical and/or cerebellar involvement on the rubral pathway.

Both motor cortex and cerebellum anticipate vibrissa position (Hill et al., 2011; Chen et al., 2016), indicating that they are part of a common network. We suspect that in intact rats rubrofacial neurons are under the joint command of both the motor cortex and the cerebellum, whereas in the absence of the motor cortex, the cerebellum is still modulating the red nucleus, contributing to the capacity to still perform the task. This possibility is made plausible by the fact that the vibrissa cerebellar cortex encodes vibrissa movement before movement occurs, even when the motor cortex is inactivated (Chen et al., 2016) and may result in cerebello-rubral synaptic sprouting. The reciprocal phenomenon, cortico-rubral sprouting, has been observed at the level of the rubrospinal pathway following cerebellar lesion (Tsukahara, 1974; Murakami et al., 1976). Interestingly, our viral labeling

reveals that rubrofacial neurons send collaterals to the lateral reticular nucleus (Fig. 10), which sends projections to the cerebellum (Qvist et al., 1984; Parenti et al., 1996; Alstermark and Ekerot, 2013). This implies that the red nucleus is sending an efference copy to the cerebellum of its motor commands to the facial nucleus (Fig. 9g). This suggests that in addition to conveying motor commands to the vibrissa motoneurons, the red nucleus may contribute to the internal representation of the vibrissa position in the cerebellum.

Our results on the dispensability of vibrissa reafference signals in intact animals are in line with the literature on eye movements, which has long demonstrated the sufficiency of efference copy in self-motion tracking (von Helmholtz, 1867; Guthrie et al., 1983). Yet, these results are at odds with the forelimb literature; studies in deafferented human patients have pointed toward accuracy deficits in limb movements (Nougier et al., 1996; Sarlegna et al., 2006; Sarlegna et al., 2010), and acutely disrupting

forelimb proprioception in mice degrades movement accuracy (Fink et al., 2014; Conner et al., 2021). However, a confounding factor prevents these forelimb results from being interpreted as implying a role for sensory feedback specifically in self-motion tracking. Indeed, forelimb muscles are load bearing, meaning that the relationship between motor commands and limb position varies depending on whether an object is handled and, if so, on the properties of the object (Gribble and Scott, 2002). Accounting for this load may constitute a necessary role of forelimb proprioception. In contrast, the vibrissa muscles are devoid of proprioceptors (Bowden and Mahran, 1956; Kleinfeld et al., 1999; Moore et al., 2015b) and, like eye muscles, are not load bearing (Guthrie et al., 1983); the same motor command results in a relatively constant muscle contraction state. Thus, our experimental model offers a new opportunity to unambiguously probe the role of internal and external feedback signals in self-motion tracking.

A wealth of behavioral and neurophysiological studies have implicated internal models in motor control in insects (Webb, 2004; Mischiati et al., 2015), rodents (Stay et al., 2019; Konosu et al., 2021), and primates (Richmond and Wurtz, 1980; Wolpert et al., 1995; Merfeld et al., 1999; Blakemore et al., 2000; Maeda et al., 2018). An internal inverse model converts a desired motor state into motor commands (Cisek, 2009; McNamee and Wolpert, 2019). The execution of a fine voluntary movement without sensory feedback implies this operation; hence, our results support the existence of an inverse model for vibrissa control. Conversely, an internal forward model estimates the state of the system, such as limb position, from internal and/or external feedback (Cisek, 2009; McNamee and Wolpert, 2019). Our results show that sensory feedback is not required in intact animals but is required in cortico-lesioned animals to maintain movement stability. These observations are consistent with the existence of a forward model relying on sensory feedback, at least in the absence of motor cortex. A related hypothesis is that the motor cortex may compensate for the absence of sensory feedback by providing the forward model with an efference copy. The central role of the cerebellum in implementing both inverse and forward models has been widely supported, from physiological to clinical studies (Wolpert et al., 1998; Shadmehr and Krakauer, 2008; Therrien and Bastian, 2015). Corticofugal projections from the motor cortex to the pontine nuclei may thus be an anatomical substrate for the transmission of cortical efference copy to a cerebellar-dependent forward model (Ishikawa et al., 2016).

References

- Ahissar E, Kleinfeld D (2003) Closed-loop neuronal computations: focus on vibrissa somatosensation in rat. *Cereb Cortex* 13:53–62.
- Alstermark B, Ekerot CF (2013) The lateral reticular nucleus: a precerebellar centre providing the cerebellum with overview and integration of motor functions at systems level. A new hypothesis. *J Physiol* 591:5453–5458.
- Berg RW, Kleinfeld D (2003) Rhythmic whisking by rat: retraction as well as protraction of the vibrissae is under active muscular control. *J Neurophysiol* 89:104–117.
- Blakemore SJ, Wolpert D, Frith C (2000) Why can't you tickle yourself? *Neuroreport* 11:R11–16.
- Bokil H, Andrews P, Kulkarni JE, Mehta S, Mitra PP (2010) Chronux: a platform for analyzing neural signals. *J Neurosci Methods* 192:146–151.
- Bowden RE, Mahran ZY (1956) The functional significance of the pattern of innervation of the muscle quadratus labii superioris of the rabbit, cat and rat. *J Anat* 90:217–227.
- Brecht M, Preilowski B, Merzenich MM (1997) Functional architecture of the mystacial vibrissae. *Behav Brain Res* 84:81–97.
- Chen S, Augustine GJ, Chadderton P (2016) The cerebellum linearly encodes whisker position during voluntary movement. *Elife* 5:e10509.
- Cheung J, Maire P, Kim J, Sy J, Hires SA (2019) The sensorimotor basis of whisker-guided anteroposterior object localization in head-fixed mice. *Curr Biol* 29:3029–3040.e4.
- Cisek P (2009) Internal models. In: *Encyclopedia of neuroscience* (Binder MD, Hirokawa N, Windhorst U (eds), pp 2009–2012. Berlin: Springer.
- Conner JM, Bohannon A, Igarashi M, Taniguchi J, Baltar N, Azim E (2021) Modulation of tactile feedback for the execution of dexterous movement. *Science* 374:316–323.
- Connolly JD, Goodale MA (1999) The role of visual feedback of hand position in the control of manual prehension. *Exp Brain Res* 125:281–286.
- Crapse TB, Sommer MA (2008) Corollary discharge across the animal kingdom. *Nat Rev Neurosci* 9:587–600.
- Curtis JC, Kleinfeld D (2009) Phase-to-rate transformations encode touch in cortical neurons of a scanning sensorimotor system. *Nat Neurosci* 12:492–501.
- Daniel H, Billard JM, Angaut P, Batini C (1987) The interposito-rubrospinal system. Anatomical tracing of a motor control pathway in the rat. *Neurosci Res* 5:87–112.
- Deschênes M, Kurnikova A, Elbaz M, Kleinfeld D (2016) Circuits in the ventral medulla that phase-lock motoneurons for coordinated sniffing and whisking. *Neural Plast* 2016:7493048.
- Ebbesen CL, Doron G, Lenschow C, Brecht M (2017) Vibrissa motor cortex activity suppresses contralateral whisking behavior. *Nat Neurosci* 20:82–89.
- Elbaz M, Callado Perez A, Demers M, Zhao S, Foo C, Kleinfeld D, Deschênes M (2022) A vibrissa pathway that activates the limbic system. *Elife* 11:e72096.
- Fee MS, Mitra PP, Kleinfeld D (1997) Central versus peripheral determinants of patterned spike activity in rat vibrissa cortex during whisking. *J Neurophysiol* 78:1144–1149.
- Fetsch CR, Odean NN, Jeurissen D, El-Shamayleh Y, Horwitz GD, Shadlen MN (2018) Focal optogenetic suppression in macaque area MT biases direction discrimination and decision confidence, but only transiently. *Elife* 7:e36523.
- Fink AJ, Croce KR, Huang ZJ, Abbott LF, Jessell TM, Azim E (2014) Presynaptic inhibition of spinal sensory feedback ensures smooth movement. *Nature* 509:43–48.
- Friedman WA, Zeigler HP, Keller A (2012) Vibrissae motor cortex unit activity during whisking. *J Neurophysiol* 107:551–563.
- Godefroy JN, Thiesson D, Pollin B, Rokyta R, Azerad J (1998) Reciprocal connections between the red nucleus and the trigeminal nuclei: a retrograde and anterograde tracing study. *Physiol Res* 47:489–500.
- Gomez JL, Bonaventura J, Lesniak W, Mathews WB, Sysa-Shah P, Rodriguez LA, Ellis RJ, Richie CT, Harvey BK, Dannals RF, Pomper MG, Bonci A, Michaelides M (2017) Chemogenetics revealed: DREADD occupancy and activation via converted clozapine. *Science* 357:503–507.
- Gribble PL, Scott SH (2002) Overlap of internal models in motor cortex for mechanical loads during reaching. *Nature* 417:938–941.
- Guo ZV, Li N, Huber D, Ophir E, Gutnisky D, Ting JT, Feng G, Svoboda K (2014) Flow of cortical activity underlying a tactile decision in mice. *Neuron* 81:179–194.
- Guthrie BL, Porter JD, Sparks DL (1983) Corollary discharge provides accurate eye position information to the oculomotor system. *Science* 221:1193–1195.
- Gutnisky DA, Yu J, Hires SA, To MS, Bale MR, Svoboda K, Golomb D (2017) Mechanisms underlying a thalamocortical transformation during active tactile sensation. *PLoS Comput Biol* 13:e1005576.
- Hattox AM, Priest CA, Keller A (2002) Functional circuitry involved in the regulation of whisker movements. *J Comp Neurol* 442:266–276.
- Henstrom D, Hadlock T, Lindsay R, Knox CJ, Malo J, Vakharia KT, Heaton JT (2012) The convergence of facial nerve branches providing whisker pad motor supply in rats: implications for facial reanimation study. *Muscle Nerve* 45:692–697.
- Herfst LJ, Brecht M (2008) Whisker movements evoked by stimulation of single motor neurons in the facial nucleus of the rat. *J Neurophysiol* 99:2821–2832.
- Hill DN, Curtis JC, Moore JD, Kleinfeld D (2011) Primary motor cortex reports efferent control of vibrissa motion on multiple timescales. *Neuron* 72:344–356.
- Isett BR, Feldman DE (2020) Cortical coding of whisking phase during surface whisking. *Curr Biol* 30:3065–3074.e5.

- Ishikawa T, Tomatsu S, Izawa J, Kakei S (2016) The cerebro-cerebellum: could it be loci of forward models? *Neurosci Res* 104:72–79.
- Isokawa-Akesson M, Komisaruk BR (1987) Difference in projections to the lateral and medial facial nucleus: anatomically separate pathways for rhythmic vibrissa movement in rats. *Exp Brain Res* 65:385–398.
- Jacquin MF, Zeigler HP (1983) Trigeminal orosensation and ingestive behavior in the rat. *Behav Neurosci* 97:62–97.
- Kleinfeld D, Deschênes M (2011) Neuronal basis for object location in the vibrissa scanning sensorimotor system. *Neuron* 72:455–468.
- Kleinfeld D, Mitra PP (2014) Spectral methods for functional brain imaging. *Cold Spring Harb Protoc* 2014:248–262.
- Kleinfeld D, Berg RW, O'Connor SM (1999) Anatomical loops and their electrical dynamics in relation to whisking by rat. *Somatosens Mot Res* 16:69–88.
- Kleinfeld D, Sachdev RN, Merchant LM, Jarvis MR, Ebner FF (2002) Adaptive filtering of vibrissa input in motor cortex of rat. *Neuron* 34:1021–1034.
- Kleinfeld D, Moore JD, Wang F, Deschênes M (2014) The brainstem oscillator for whisking and the case for breathing as the master clock for orofacial motor actions. *Cold Spring Harb Symp Quant Biol* 79:29–39.
- Knutsen PM, Pietr M, Ahissar E (2006) Haptic object localization in the vibrissal system: behavior and performance. *J Neurosci* 26:8451–8464.
- Konosu A, Funato T, Matsuki Y, Fujita A, Sakai R, Yanagihara D (2021) A model of predictive postural control against floor tilting in rats. *Front Syst Neurosci* 15:785366.
- Lavallée P, Urbain N, Dufresne C, Bokor H, Acsády L, Deschênes M (2005) Feedforward inhibitory control of sensory information in higher-order thalamic nuclei. *J Neurosci* 25:7489–7498.
- Maeda RS, Cluff T, Gribble PL, Pruszynski JA (2018) Feedforward and feedback control share an internal model of the arm's dynamics. *J Neurosci* 38:10505–10514.
- Mahler SV, Aston-Jones G (2018) CNO evil? Considerations for the use of DREADDs in behavioral neuroscience. *Neuropsychopharmacology* 43:934–936.
- Manvich DF, Webster KA, Foster SL, Farrell MS, Ritchie JC, Porter JH, Weinschenker D (2018) The DREADD agonist clozapine N-oxide (CNO) is reverse-metabolized to clozapine and produces clozapine-like interoceptive stimulus effects in rats and mice. *Sci Rep* 8:3840.
- Mao T, Kusefoglu D, Hooks BM, Huber D, Petreanu L, Svoboda K (2011) Long-range neuronal circuits underlying the interaction between sensory and motor cortex. *Neuron* 72:111–123.
- McElvain LE, Friedman B, Karten HJ, Svoboda K, Wang F, Deschênes M, Kleinfeld D (2018) Circuits in the rodent brainstem that control whisking in concert with other orofacial motor actions. *Neuroscience* 368:152–170.
- McNamee D, Wolpert DM (2019) Internal models in biological control. *Annu Rev Control Robot Auton Syst* 2:339–364.
- Mehta SB, Whitmer D, Figueroa R, Williams BA, Kleinfeld D (2007) Active spatial perception in the vibrissa scanning sensorimotor system. *PLoS Biol* 5:e15.
- Merfeld DM, Zupan L, Peterka RJ (1999) Humans use internal models to estimate gravity and linear acceleration. *Nature* 398:615–618.
- Mischianti M, Lin HT, Herold P, Imler E, Olberg R, Leonardo A (2015) Internal models direct dragonfly interception steering. *Nature* 517:333–338.
- Moore JD, Deschênes M, Furuta T, Huber D, Smear MC, Demers M, Kleinfeld D (2013) Hierarchy of orofacial rhythms revealed through whisking and breathing. *Nature* 497:205–210.
- Moore JD, Deschênes M, Kleinfeld D (2015a) Juxtacellular monitoring and localization of single neurons within sub-cortical brain structures of alert, head-restrained rats. *J Vis Exp* 2015:51453.
- Moore JD, Mercer Lindsay N, Deschênes M, Kleinfeld D (2015b) Vibrissa self-motion and touch are reliably encoded along the same somatosensory pathway from brainstem through thalamus. *PLoS Biol* 13:e1002253.
- Murakami F, Fujito Y, Tsukahara N (1976) Physiological properties of the newly formed cortico-rubral synapses of red nucleus neurons due to colateral sprouting. *Brain Res* 103:147–151.
- Nougier V, Bard C, Fleury M, Teasdale N, Cole J, Forget R, Paillard J, Lamarre Y (1996) Control of single-joint movements in deafferented patients: evidence for amplitude coding rather than position control. *Exp Brain Res* 109:473–482.
- O'Connor DH, Clack NG, Huber D, Komiyama T, Myers EW, Svoboda K (2010) Vibrissa-based object localization in head-fixed mice. *J Neurosci* 30:1947–1967.
- O'Connor SM, Berg RW, Kleinfeld D (2002) Coherent electrical activity between vibrissa sensory areas of cerebellum and neocortex is enhanced during free whisking. *J Neurophysiol* 87:2137–2148.
- Otchy TM, Wolff SB, Rhee JY, Pehlevan C, Kawai R, Kempf A, Gobes SM, Ólveczky BP (2015) Acute off-target effects of neural circuit manipulations. *Nature* 528:358–363.
- Pacheco-Calderón R, Carretero-Guillen A, Delgado-García JM, Gruart A (2012) Red nucleus neurons actively contribute to the acquisition of classically conditioned eyelid responses in rabbits. *J Neurosci* 32:12129–12143.
- Parenti R, Cicirata F, Pantò MR, Serapide MF (1996) The projections of the lateral reticular nucleus to the deep cerebellar nuclei. An experimental analysis in the rat. *Eur J Neurosci* 8:2157–2167.
- Petreanu L, Gutnisky DA, Huber D, Xu NL, O'Connor DH, Tian L, Looger L, Svoboda K (2012) Activity in motor-sensory projections reveals distributed coding in somatosensation. *Nature* 489:299–303.
- Qvist H, Dietrichs E, Walberg F (1984) An ipsilateral projection from the red nucleus to the lateral reticular nucleus in the cat. *Anat Embryol (Berl)* 170:327–330.
- Ranganathan GN, Apostolides PF, Harnett MT, Xu NL, Druckmann S, Magee JC (2018) Active dendritic integration and mixed neocortical network representations during an adaptive sensing behavior. *Nat Neurosci* 21:1583–1590.
- Richmond BJ, Wurtz RH (1980) Vision during saccadic eye movements. II. A corollary discharge to monkey superior colliculus. *J Neurophysiol* 43:1156–1167.
- Sarlegna FR, Gauthier GM, Bourdin C, Vercher JL, Blouin J (2006) Internally driven control of reaching movements: a study on a proprioceptively deafferented subject. *Brain Res Bull* 69:404–415.
- Sarlegna FR, Malfait N, Bringoux L, Bourdin C, Vercher JL (2010) Force-field adaptation without proprioception: can vision be used to model limb dynamics? *Neuropsychologia* 48:60–67.
- Severson KS, Xu D, Van de Loo M, Bai L, Ginty DD, O'Connor DH (2017) Active touch and self-motion encoding by merkel cell-associated afferents. *Neuron* 94:666–676.e9.
- Severson KS, Xu D, Yang H, O'Connor DH (2019) Coding of whisker motion across the mouse face. *Elife* 8:e41535.
- Shadmehr R, Krakauer JW (2008) A computational neuroanatomy for motor control. *Exp Brain Res* 185:359–381.
- Sreenivasan V, Karmakar K, Rijli FM, Petersen CC (2015) Parallel pathways from motor and somatosensory cortex for controlling whisker movements in mice. *Eur J Neurosci* 41:354–367.
- Sreenivasan V, Esmaeili V, Kiritani T, Galan K, Crochet S, Petersen CCH (2016) Movement initiation signals in mouse whisker motor cortex. *Neuron* 92:1368–1382.
- Stay TL, Laurens J, Sillitoe RV, Angelaki DE (2019) Genetically eliminating Purkinje neuron GABAergic neurotransmission increases their response gain to vestibular motion. *Proc Natl Acad Sci U S A* 116:3245–3250.
- Takato J, Nelson A, Zhou X, Bolton MM, Ehlers MD, Arenkiel BR, Mooney R, Wang F (2013) New modules are added to vibrissal premotor circuitry with the emergence of exploratory whisking. *Neuron* 77:346–360.
- Takato J, Prevosto V, Thompson PM, Lu J, Chung L, Harrahill A, Li S, Zhao S, He Z, Golomb D, Kleinfeld D, Wang F (2022) The whisking oscillator circuit. *Nature* 609:560–568.
- Therrien AS, Bastian AJ (2015) Cerebellar damage impairs internal predictions for sensory and motor function. *Curr Opin Neurobiol* 33:127–133.
- Tsukahara N (1974) Sprouting of cortico-rubral synapses in red nucleus neurons after destruction of the nucleus interpositus of the cerebellum. *Experientia* 30:57–58.
- Urbain N, Salin PA, Libourel PA, Comte JC, Gentet LJ, Petersen CCH (2015) Whisking-related changes in neuronal firing and membrane potential dynamics in the somatosensory thalamus of awake mice. *Cell Rep* 13:647–656.
- Vaidya AR, Pujara MS, Petrides M, Murray EA, Fellows LK (2019) Lesion studies in contemporary neuroscience. *Trends Cogn Sci* 23:653–671.
- Veinante P, Deschênes M (2003) Single-cell study of motor cortex projections to the barrel field in rats. *J Comp Neurol* 464:98–103.
- von Helmholtz H, (1867) *Handbuch der physiologischen Optik*. Leipzig, Germany: Voss.

- Wallach A, Bagdasarian K, Ahissar E (2016) On-going computation of whisking phase by mechanoreceptors. *Nat Neurosci* 19:487–493.
- Webb B (2004) Neural mechanisms for prediction: do insects have forward models? *Trends Neurosci* 27:278–282.
- Welker WI (1964) Analysis of sniffing of the albino rat. *Behaviour*, Leiden 22:223–244.
- Wolff SB, Ölveczky BP (2018) The promise and perils of causal circuit manipulations. *Curr Opin Neurobiol* 49:84–94.
- Wolpert DM, Ghahramani Z (2000) Computational principles of movement neuroscience. *Nat Neurosci* 3 Suppl:1212–1217.
- Wolpert DM, Ghahramani Z, Jordan MI (1995) An internal model for sensorimotor integration. *Science* 269:1880–1882.
- Wolpert DM, Miall RC, Kawato M (1998) Internal models in the cerebellum. *Trends Cogn Sci* 2:338–347.
- Wurtz RH (2018) Corollary discharge contributions to perceptual continuity across saccades. *Annu Rev Vis Sci* 4:215–237.
- Yu C, Derdikman D, Haidarliu S, Ahissar E (2006) Parallel thalamic pathways for whisking and touch signals in the rat. *PLoS Biol* 4:e124.
- Zhu H, Roth BL (2014) Silencing synapses with DREADDs. *Neuron* 82:723–725.
- Zucker E, Welker WI (1969) Coding of somatic sensory input by vibrissae neurons in the rat's trigeminal ganglion. *Brain Res* 12:138–156.